A Phase Diagram Approach to Study Liquation Cracking in Alloy 718

B. RADHAKRISHNAN and R.G. THOMPSON

The constitutional liquation of NbC wrought alloy 718 is discussed in terms of a diffusion couple between NbC and the γ matrix in a pseudo-ternary of γ-NbC-Laves. Theoretical arguments are presented to show that the diffusion path cannot be a straight line connecting the terminal compositions. Experimental results indicate the existence of the NbC-γ diffusion couple and also support the hypothesis that the diffusion path is not a straight line connecting NbC and γ. Consequently, the temperature at which carbide liquation can occur is below the equilibrium NbC solidus, and hence, carbide liquation is constitutional in nature. The lowest temperature at which carbide liquation initiates depends upon the extent of deviation of the diffusion path from the straight line path. The dependence of the relative volume fractions of carbide and Laves phase in cast alloys on Nb/C ratio is explained using the γ-NbC-Laves pseudo-ternary. The Laves phase present in cast alloys is shown to liquate at the terminal eutectic temperature of the alloy, which could be lower than the carbide liquation temperature.

I. INTRODUCTION

INTERGRANULAR liquation and cracking in the weld heat-affected zone (HAZ) is a phenomenon encountered in several alloy systems. This phenomenon is also referred to as microfissuring and intergranular hot cracking. Some of the alloy systems in which liquation cracking is observed and the corresponding liquating phases are shown in Table I.[1–5] The combination of liquid films along grain boundaries and thermal stress due to the weld thermal cycle can lead to the formation of intergranular cracks. The mechanism by which liquid forms has been attributed to the constitutional liquation of certain precipitates, a mechanism first proposed by Pepe and Savage.[6]

Constitutional liquation can be illustrated with the help of a simple binary eutectic shown in Figure 1. Alloy C_0 has a certain volume fraction of second-phase particles, AB, at room temperature. When the alloy is rapidly heated to a temperature, T, above the binary eutectic temperature, T_E, there may be insufficient time for complete dissolution of AB. Hence, at temperatures above T_E, the AB phase is still present. Dissolution of AB above T_E takes place by the formation of a liquid phase which subsequently resolidifies in accordance with phase diagram requirements. The concentration gradients in the matrix adjacent to the AB particle are shown in Figure 1(b). The terms C_{l_1} and C_{l_2} are the concentrations of liquid in equilibrium with γ and AB, respectively, at temperature T. The term C_s is the concentration of γ in equilibrium with liquid, and C_m is the concentration of the γ matrix in equilibrium with the AB particle at room temperature.

In alloy 718, the formation of liquid has been attributed to the constitutional liquation of NbC particles,[1,7] Laves phase[8,9,10] and possibly minority phases, such as silicides[10] or borides,[10,11] in wrought alloys. In cast as well as wrought alloys, the carbides were known to liquate at a higher temperature than the Laves phase.[8,9] Even though these experimental results are fairly well established, there have been no attempts to offer a unified theory of liquation of the various phases in alloy 718 with respect to a common phase diagram. While the constitutional liquation of a second phase in a binary system can be easily explained by using the phase diagram, the approach becomes quite complicated when the complex phase relationships involved in a multicomponent system are considered. However, simplified pseudo-ternary diagrams can be constructed for multicomponent systems from a knowledge of the solidification sequence of the alloy and microstructural information.

Eiselstein[12] was the first to develop a constitutional diagram for the final stages of solidification of alloy 718. The final event of solidification was represented as a binary eutectic involving the γ phase and Laves phase. This diagram was recently modified by Knorovsky *et al.*[13] and Bouse.[14] The binary representation of the final event of solidification, although capable of explaining the eutectic melting of the Laves phase in cast alloys, cannot explain the constitutional liquation of NbC in wrought alloys. Radhakrishnan and Thompson[15] modified the solidification sequence developed by Knorovsky *et al.* and developed the γ-NbC-Laves pseudo-ternary for alloy 718 shown in Figure 2. The final solidification event was considered as a ternary eutectic of $L \rightarrow \gamma + NbC +$ Laves rather than a binary eutectic, in agreement with the precipitate morphologies of resolidified grain boundary liquid reported by Vincent.[16] The pseudo-ternary model allowed for the formation of NbC over a range of temperatures, as required for a monovariant reaction.

The objective of the present study is to show that such a model can be used to explain the constitutional liquation of NbC in wrought alloys and the liquation of Laves phase in cast alloys.

II. EXPERIMENTAL WORK

The alloy compositions used in this study are shown in Table II. Table III summarizes the heat treatments used.

B. RADHAKRISHNAN, Postdoctoral Fellow, and R.G. THOMPSON, Professor, are with the Department of Materials Science and Engineering, University of Alabama at Birmingham, Birmingham, AL 35294.

Manuscript submitted August 14, 1989.

Table I. Constitutional Liquation in Multicomponent Systems

Alloy System	Liquating Phase	Reference
HASTELLOY* X	M_6C	Duvall and Owczarski[1]
INCONEL** 600	Cr_7C_3, Ti(CN)	Weiss *et al.*[2]
18 pct Maraging steel	titanium sulfide	Pepe and Savage[3]
Austenitic alloy A286	TiC or Ti(CN)	Brooks[4]
High-strength Mg base alloy	Nd, Y-containing phase	Baeslack III *et al.*[5]

*HASTELLOY is a trademark of Stoady Deloro Stellite, Inc., Industry, CA.
**INCONEL is a trademark of Inco Alloys International, Inc., Huntington, WV.

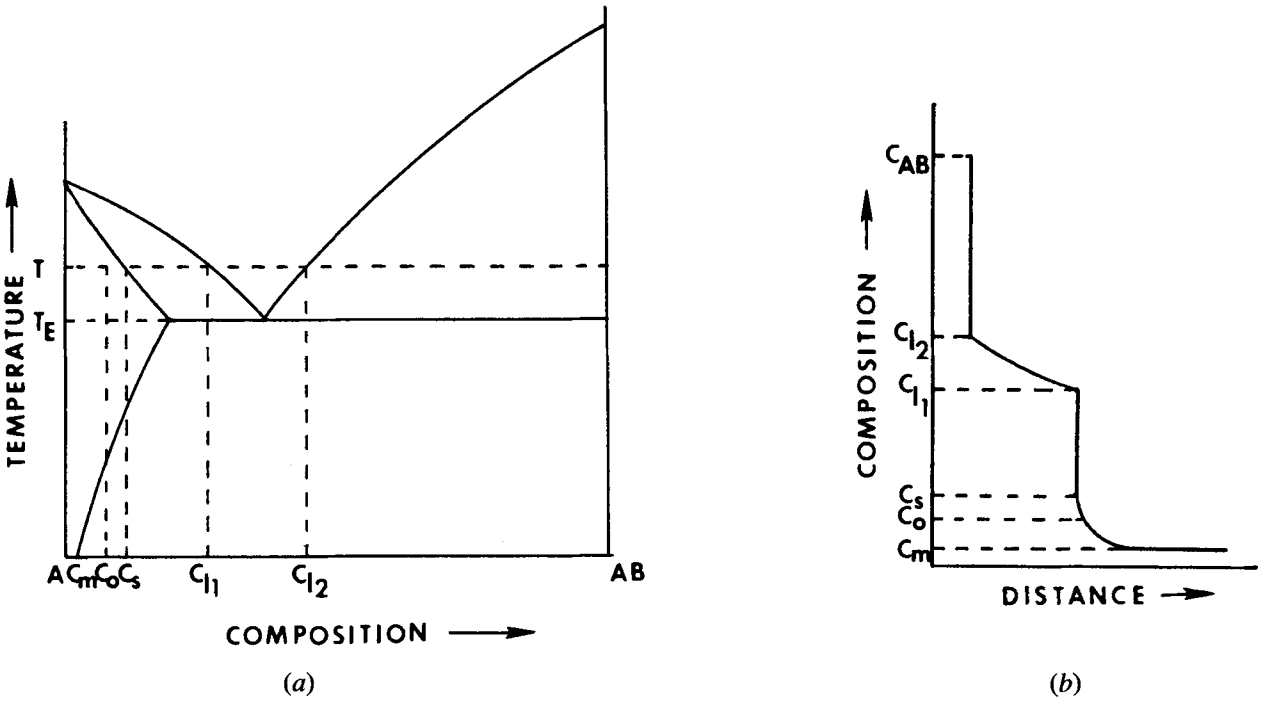

(*a*) (*b*)

Fig. 1—(*a*) Schematic of constitutional liquation of *AB* particle in a binary system and (*b*) concentration gradients in front of the liquating *AB* particle.

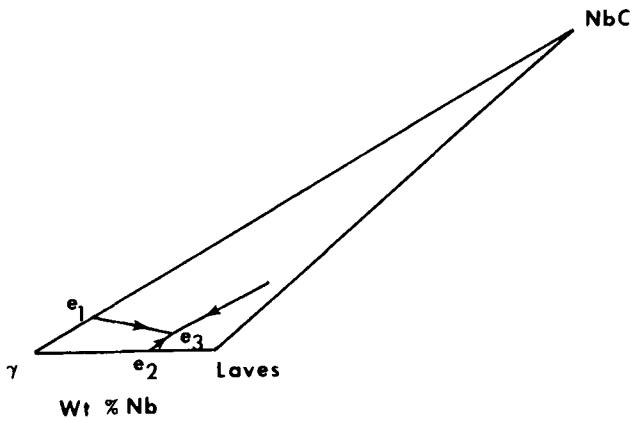

Fig. 2—Schematic of the pseudo-ternary γ-NbC-Laves. The eutectic e_1 is similar to the γ-NbC eutectic reported by Knorovsky *et al.*[13] The eutectic e_2 is the true binary eutectic between γ and Laves, which is not known; e_3 is the ternary eutectic of γ, Laves, and NbC.[15]

Table II. Alloy Compositions

Elements	Alloy 1 (Wt Pct)	Alloy 2 (Wt Pct)	Alloy 3 (Wt Pct)
Cr	18.12	19.5	19.5
Fe	19.07	bal.	bal.
Ni	53.24	52.4	52.2
Mn	0.07	< 0.05	< 0.01
Cb + Ta	5.0	5.0	4.70
Cu	0.05	< 0.05	< 0.05
C	0.03	0.06	0.021
Mo	2.28	3.0	3.0
Si	0.11	0.02	0.008
Al	0.52	0.55	0.56
Ti	0.94	1.02	1.01
Co	0.09	< 0.10	< 0.01
B	0.003	0.004	0.003
S	0.001	0.0008	0.0008

Table III. Summary of Heat Treatments

Alloy	Heat Treatment
Alloy 1 (wrought)	heated to 1093 °C at approximately 125 °C/s, held for 100 s, and quenched to room temperature
Alloy 1 (wrought)	homogenized at 1093 °C for 15 min in Ar atmosphere, followed by air cooling
Alloy 2 (cast)	homogenized at 1093 °C for 1 h in Ar atmosphere, air cooled to room temperature, homogenized at 1093 °C in air for 10 min, and air cooled to room temperature
Alloy 3 (cast)	same as Alloy 2

Alloy 1 was in the form of hot-rolled rods 5 mm in diameter, from which Gleeble samples 90 mm long with a gage length of 24 mm were prepared. Gleeble samples of alloys 2 and 3 were in the form of strips 90 × 4 × 1.5 mm in dimension. These strips were machined from a cast bar 250 × 25 × 4 mm in dimension. Gleeble samples of alloys 2 and 3 were heat-treated first in a tube furnace in an argon atmosphere for 1 hour, followed by an additional heat treatment in a muffle furnace for 10 minutes in air. The 1-hour heat treatment at 1093 °C is the typical homogenization heat treatment for cast 718 alloys. The present study was part of a greater research program concerning the effect of homogenization on the hot-cracking susceptibility of cast alloy 718. The purpose of the second heat treatment in air was to form a black oxide coating with an emissivity of about 0.9. Gleeble samples of alloy 1 were heat-treated in the Gleeble in air for 100 seconds. These samples also had a black oxide coating similar to the coatings found on samples of alloys 2 and 3. This heat treatment also resulted in the dissolution of the δ phase (Ni_3Nb) present in alloy 1 in the as-received condition.

The accurate measurement of sample temperature during thermal simulation in a Gleeble poses certain problems, especially when small sample sizes are used. In the present study, the dimensions of the Gleeble samples were limited by the availability of material. Because of the small sample size, the heat loss by conduction through the thermocouple percussion welded to the sample was large enough to locally reduce the sample temperature. Hence, it was decided to use an optical pyrometer which senses the radiative output of the sample, thereby eliminating the heat loss by conduction through the thermocouple. The temperature control circuit was modified to include an IRCON* Modline (Series 6000) radiation pyrometer with a temperature capability of 1650 °C as the control unit. The pyrometer had an auxiliary output of 0 to 100 mv DC, which was used as the feedback signal for temperature control. The response time at this auxiliary output was 0.1 seconds for 95 pct of full-scale input, which was considered sufficiently short for this application. The pyrometer was calibrated using the following procedure.

*IRCON is a trademark of Ircon, Inc., Niles, IL.

A Gleeble sample of alloy 718 of a given geometry was prepared and a type K thermocouple (0.25 mm in diameter) was percussion welded to the midsection of the sample gage length. The cross section of the Gleeble sample was several orders of magnitude larger than the cross section of the thermocouple wire, so that the heat loss due to conduction was minimized. The optical pyrometer was focused on the Gleeble sample as closely as possible to the spot where the thermocouple leads were welded. The emissivity setting on the pyrometer was set to a constant value of 0.9. The sample was subjected to a given thermal cycle. The thermal cycle used for calibration was identical to the one used in later experiments. The outputs of the thermocouple and the pyrometer were measured using a Kipp & Zonen BD-40 strip chart recorder. This procedure was repeated for several thermal cycles of increasing peak temperatures. The time to reach peak temperature was kept constant for all of the thermal cycles. A calibration curve, as shown in Figure 3, was generated. The variation in the thermocouple output was within ±0.1 mV for a given sample when heated to any particular temperature represented by the pyrometer output. However, there was a greater variation in thermocouple output from one sample to another, probably due to variations in the quality of the percussion weld and the focusing of the pyrometer circle on the sample closest to the thermocouple. The overall variation at any temperature did not exceed ±15 °C.

When a machined sample which had a bright surface was used, the temperature recorded by the thermocouple for a given millivolt output of the pyrometer was not constant for the first few cycles. This was due to the low emissivity of the machined sample (0.15). However, after a few cycles, the thermocouple output stabilized to a constant lower value as the sample surface was covered by a black oxide which had a constant emissivity of about 0.9. Subsequent runs were made with the pyrometer as the controlling unit. Since all Gleeble samples had a tenacious black oxide coating of constant emissivity, no

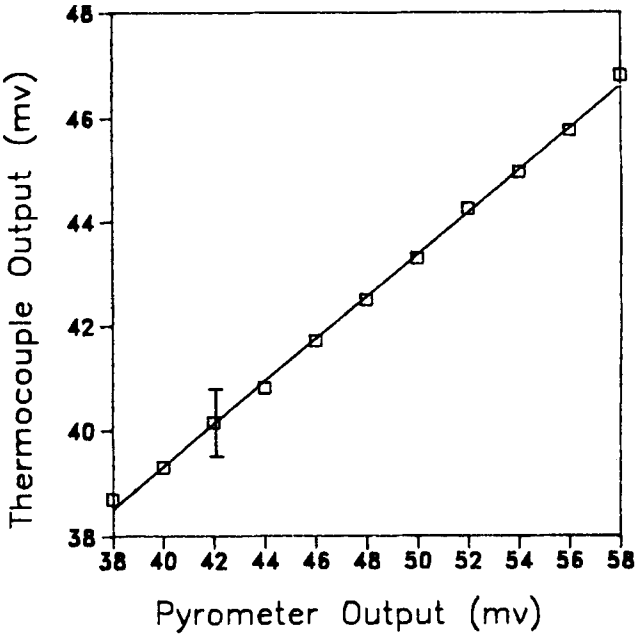

Fig. 3—Calibration curve for the optical pyrometer. The error bar corresponds to a temperature variation of ±15 °C.

errors were encountered due to emissivity variation during the test. In order to check the accuracy of temperature measurement using the pyrometer, samples of alloy 1 were subjected to similar thermal simulations by using an extremely fine wire (0.075-mm diameter) type K thermocouple as the temperature measurement and control unit. The thermal cycle used for the Gleeble simulations is shown in Figure 4. The samples were heated to the peak temperatures in about 8 seconds and quenched to room temperature. Three peak temperatures (1190 °C, 1215 °C, and 1235 °C) were used for each of the alloy heats.

For alloys 1 through 3 run with pyrometer control, the gage length portion of the Gleeble samples was mounted longitudinally and prepared for metallographic examination. For samples run with thermocouple control, transverse sections containing the thermocouple junction were examined. Samples were prepared by using conventional grinding and polishing techniques and etched electrolytically in 10 pct oxalic acid for 5 seconds at 6 V at room temperature. Scanning electron microscopy (SEM) studies were carried out in a PHILIPS* 515 scanning electron microscope.

*PHILIPS is a trademark of Philips Electronic Instruments Corporation, Mahwah, NJ.

Thin foils for transmission electron microscopy (TEM) were prepared from a Gleeble sample of alloy 1 heated to a peak temperature of 1227 °C by using thermocouple control and quenched from the peak temperature. Discs 3 mm in diameter and 100 μm in thickness were prepared by using Gatan grinding equipment. Jet polishing was carried out in a Struers Tenupol 2 electropolishing unit by using an electrolyte consisting of perchloric acid, methanol, and butyl cellusolve at an operating temperature of −45 °C at 45 V. Composition profile across a liquating carbide was obtained using a JEOL 2000FX transmission electron microscope fitted with a KEVEX* 8000 energy dispersive spectroscopy (EDS) system at an accelerating voltage of 200 kV. Spectral analysis was carried out using Quantex software. The EDS results are shown in Table IV and in Figures 19 and 20. It must be mentioned that the purpose of the analytical electron microscopy (AEM) study reported here was not to measure the absolute elemental concentrations of phases but to measure the relative concentration gradients that might exist between the liquating carbides and the matrix. Quantification was carried out using thin film approximation and theoretically calculated k-ratios. It is known that the relative error introduced by the use of theoretical k-ratios could be as high as ±15 pct.[17] The relative error due to counting was calculated as $3[(N_A)^{-1/2} + (N_B)^{-1/2}]$, where N_A and N_B were the total counts for elements A and B, respectively, after background subtraction. The absorption correction factor[17] for all of the k-ratios was less than ±5 pct for sample thicknesses up to 500 nm. The sample was electron-transparent down to 100 keV and, hence, was considered thin enough to neglect absorption and fluorescence corrections. However, because of the above sources of error, the accuracy of the concentrations reported here may be only ±20 pct. The error bars shown in Figures 19 and 20 represent only the statistical error due to counting and not the errors introduced due to uncertainties in the calculation of the theoretical k-ratios.[17] The spectra were collected using an automatic stepping procedure. Each spectrum was collected for a period of 200 live seconds. The total counts for Cr, Fe, and Ni were 10,000 at all locations except the carbides. However, the counts for Ti and Mo were generally of the order of 750 to 1000 only because of the low concentration of these elements. The Nb count was greater than 100,000 on the carbides, about 10,000 to 15,000 on the liquid, and ranged from about 7500 at the liquid-matrix interface to about 1500 in the matrix well away from the liquid-matrix interface. Figures 19 and 20 indicate the presence of elemental concentration gradients in front of the liquating carbide.

*KEVEX is a trademark of Kevex Corporation, Foster City, CA.

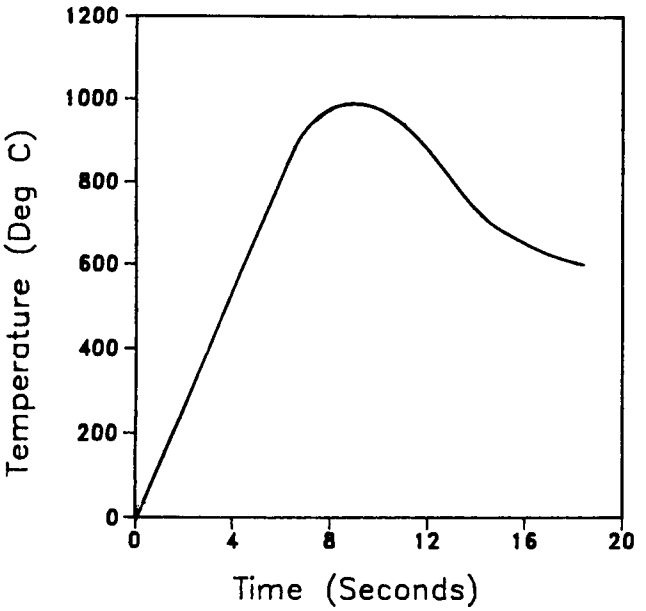

Fig. 4—Typical Gleeble thermal cycle used in this study. The time taken to reach peak temperature was kept constant at about 8.0 s for the three peak temperatures used.

III. RESULTS

A. *Wrought Alloy*

The microstructures of alloy 1 in the as-received condition and after heat treatment in the Gleeble for 100 seconds at 1093 °C are shown in Figure 5. The relief effects seen in Figure 5(b) are due to the dissolution of the δ phase present in the as-received microstructure. Figure 6 shows the microstructure of the heat-treated sample after thermal cycling to a temperature of 1235 °C. Since there was a temperature gradient in the Gleeble sample, there was a gradual change in the appearance of the grain boundaries and carbides as the peak temperature portion of the Gleeble sample was approached.

Figure 7 shows the extreme left microstructure of Figure 6 at higher magnifications. Adjacent to the grain-boundary carbides (G) and interior carbides (I), there is

Table IV. Transmission Electron Microscopy Energy Dispersive Spectroscopy Analysis of Phases*

Location	(Wt Pct) Ti	Cr	Fe	Ni	Nb	Mo
Carbide (this study)	3.7	0.6	0.6	1.7	92.1	1.3
Liquid in contact with carbide (max. Nb) (this study)	1.3	11.2	10.3	39.9	31.5	5.8
Laves phase (Knorovsky *et al.*)[13]	1.1	13.0	11.6	45.2	22.4	4.9
Matrix adjacent to liquid (this study)	1.5	16.1	15.5	52.4	10.3	4.3
Eutectic γ (Knorovsky *et al.*)[13]	1.7	14.2	12.8	58.3	9.3	3.4
Matrix 1 mm away from edge of liquid (this study)	1.0	17.6	17.9	52.6	6.7	4.3

*The relative error in the elemental concentrations reported in this study is about ±20 pct, which is the sum of the error due to counting and the relative error in the *k*-ratios. The relative error in the values reported by Knorovsky *et al.*[13] is ±5 pct.

quenched-in liquid.* The liquid adjacent to grain-boundary carbides partially wetted the grain boundaries. The interior carbides were also partially liquated. The sample quenched from a peak temperature of 1215 °C had a microstructure identical to that of Figure 7, showing the initiation of carbide liquation at 1215 °C. Figures 8 and 9 show the progressive increase in the degree of carbide

*"Quenched-in liquid" refers to the volume of resolidified material which, just prior to quenching, was liquid.

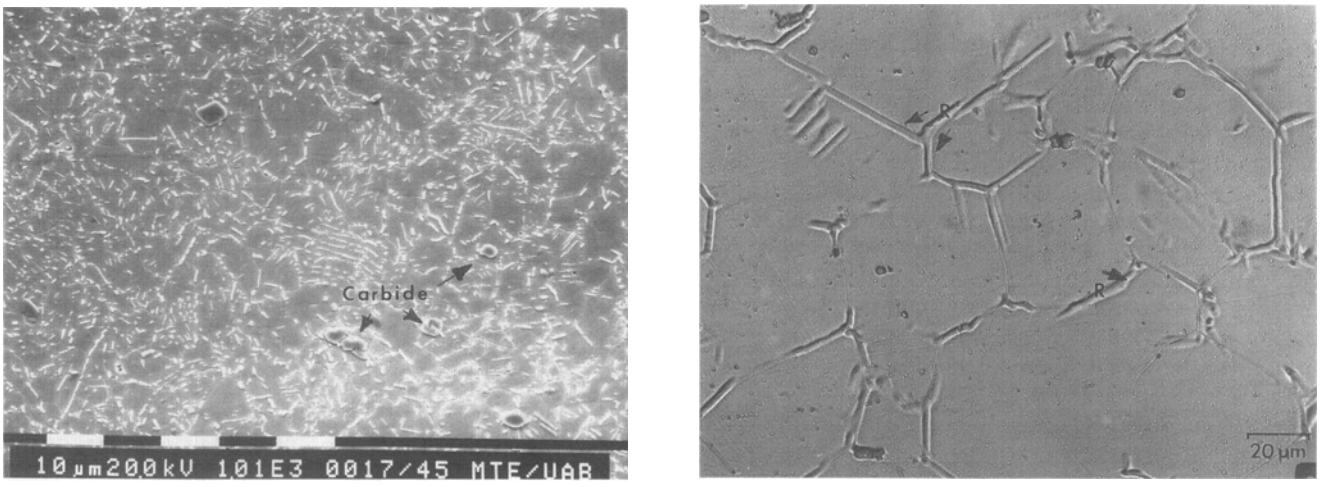

(*a*) (*b*)

Fig. 5—(*a*) Microstructure of alloy 1 in the as-received condition consisting of carbides and Ni_3Nb in the γ matrix. (*b*) Microstructure after a 100-s hold at 1093 °C. The plates of δ initially present in the microstructure have dissolved, giving rise to relief effects (R).

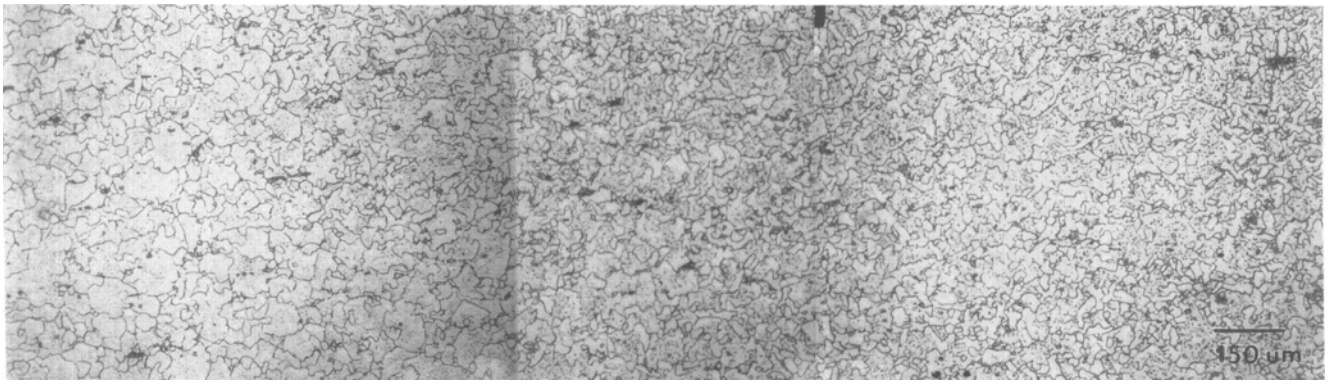

Fig. 6—Microstructure of the wrought alloy at various locations of the Gleeble sample quenched from 1235 °C. The extreme left corresponds to the beginning of liquation (approximately 1215 °C), and the extreme right corresponds to liquation at the peak temperature (1235 °C).

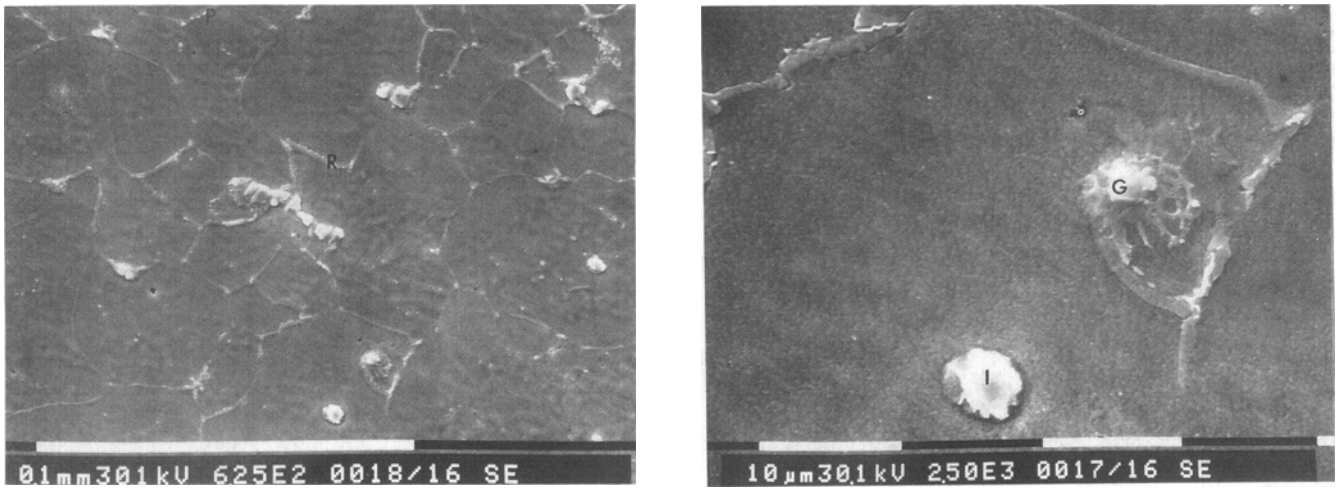

(*a*) (*b*)

Fig. 7—(*a*) Extreme left microstructure of Fig. 6, showing beginning of carbide liquation. There are some isolated regions of resolidified liquid (P) on grain boundaries remote from carbides. (*b*) Liquation of grain-boundary carbides (G) and interior carbides (I) shown at higher magnification.

liquation and spreading of the grain-boundary liquid as the peak temperature portion of the gage length is approached from either end. The peak temperature zone (1235 °C) of the Gleeble sample is shown in Figure 10. All of the carbides have totally liquated, and the liquid has spread to cover almost all of the grain boundaries.

In Figures 7 through 10, there appears to be liquid along certain boundaries which apparently do not have liquating carbides in their near vicinity. While it is possible that some of the liquating carbides contributing to the above grain-boundary liquation may be situated below the plane of polish, it appears that the volume fraction of the grain-boundary liquid in any random section is more than the volume fraction of liquid that can form from the coarse liquating carbides in that section.

Figure 11 shows the microstructure of alloy 1 initially homogenized for 15 minutes at 1093 °C, heated to a peak temperature of 1200 °C using thermocouple control. Notice the initiation of liquation at the carbide-matrix interface. Figure 12 shows the microstructure of alloy 1 in the as-received condition heated to a peak temperature of 1227 °C using thermocouple control. Notice the complete liquation of the carbides at this temperature. The microstructures shown in Figures 11 and 12 were obtained from transverse sections containing the thermocouple at a radial distance of 0.5 mm from the surface. Hence, any errors due to longitudinal and transverse temperature gradients in the sample were minimized.

B. *Cast Alloys*

The microstructures of the cast alloys 2 and 3 are shown in Figures 13 and 14, respectively. Alloy 2, which had a higher C/Nb ratio, had a larger carbide/Laves ratio than alloy 3. Figure 15 shows a longitudinal section of a Gleeble sample of alloy 2. At the extreme left, corresponding to the beginning of liquation, both intergranular and intragranular Laves phases have liquated.

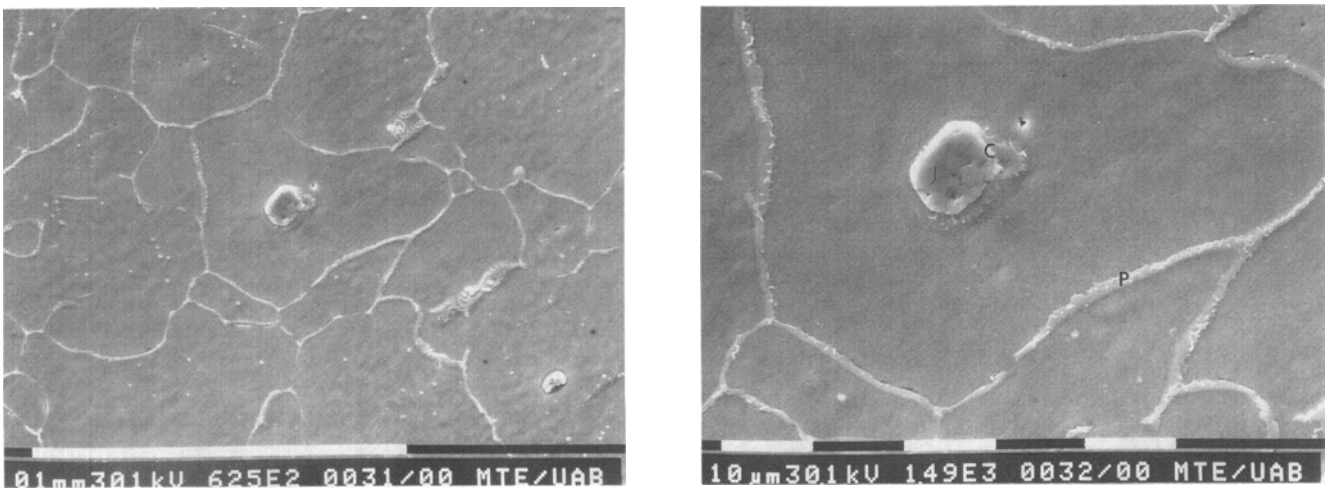

(*a*) (*b*)

Fig. 8—(*a*) Liquation of carbides in a region where the peak temperature was slightly higher than in Fig. 7. (*b*) Higher magnification of region shown in (a), showing carbide liquation (C) and an increase in the volume fraction of the resolidified liquid (P) remote from the carbides.

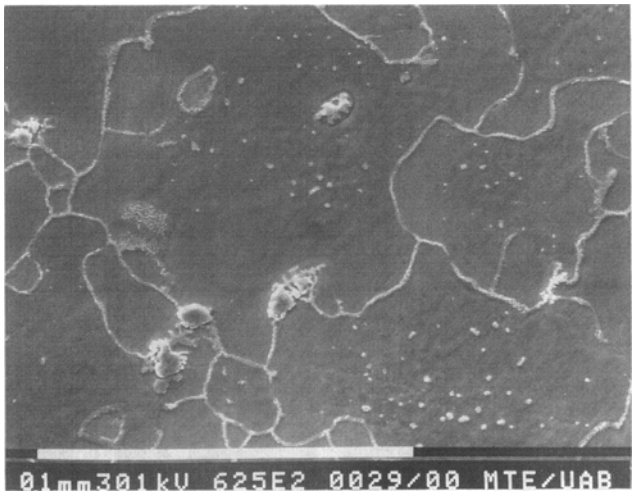

(*a*)

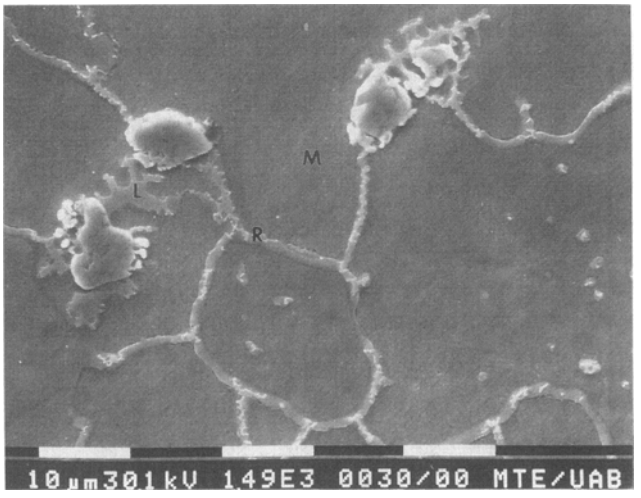

(*b*)

Fig. 9—(*a*) Region where peak temperature was higher than in Fig. 8, showing more extensive liquation of grain boundary and interior carbides, and (*b*) the spreading of the grain-boundary liquid. The liquated boundaries show a surface relief (R) which is not found in the matrix (M) away from the grain boundaries. The liquid around the carbides is marked "L."

The carbides in these regions apparently remain unaffected. Figure 16 shows the extent of liquation for alloys 2 and 3 when quenched from 1215 °C, the temperature corresponding to the extreme left of Figure 15. At the extreme right, corresponding to the peak temperature of the Gleeble sample (1235 °C), the carbide liquation is more extensive, as shown in Figure 17.

Figure 18 shows the TEM bright-field image of a liquated carbide from a transverse section situated at the midsection of the Gleeble sample. Composition profiles across the liquated carbide, liquid, and the matrix adjacent to the liquid are shown in Figure 19. A composition profile across the edge of the liquid and the adjacent matrix is shown in Figure 20. Typical compositions of carbide, liquid, and matrix are shown in Table IV.

IV. DISCUSSION

Two important observations can be made from the liquation behavior of the wrought and cast 718 alloys of this study. First, liquation of the carbides in the wrought alloys initiated at a temperature of 1200 °C to 1215 °C, which was well below the γ-carbide eutectic temperature of 1250 °C.[13] The extent of carbide liquation continued to increase at higher peak temperatures and was complete at a peak temperature of 1235 °C. This implies that the carbides liquate over a range of temperatures rather than at a single temperature. It may be argued that the observation of a melting range for NbC could be a kinetic effect. However, studies of isothermal carbide liquation[18] clearly showed that complete carbide liquation

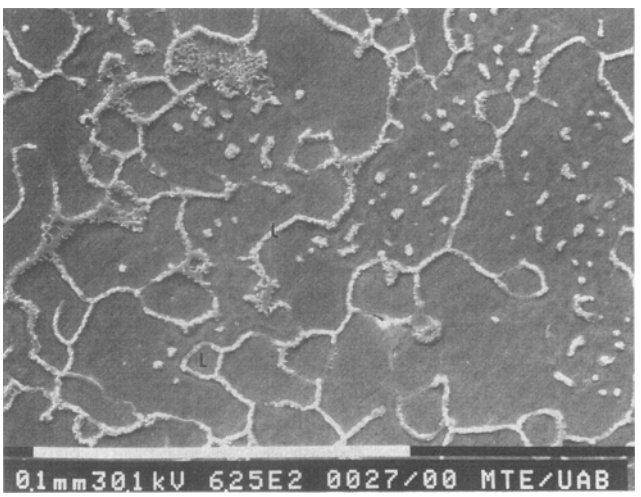

(*a*)

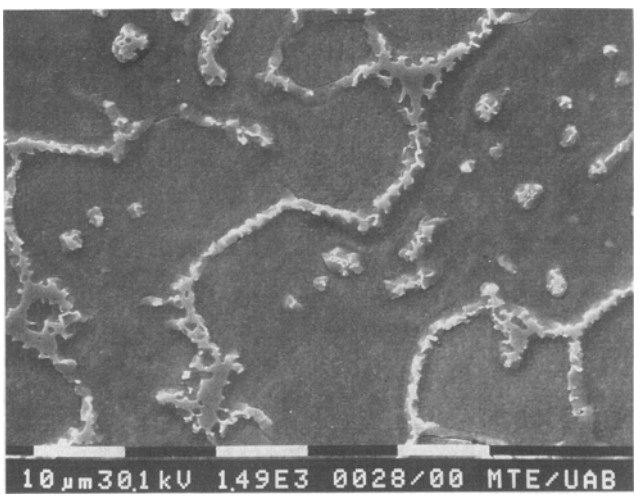

(*b*)

Fig. 10—(*a*) Liquation at the center of the Gleeble sample, where the peak temperature was 1235 °C, showing complete liquation of the carbides and the presence of continuous grain-boundary liquid (L). (*b*) Higher magnification micrograph of the grain-boundary liquid.

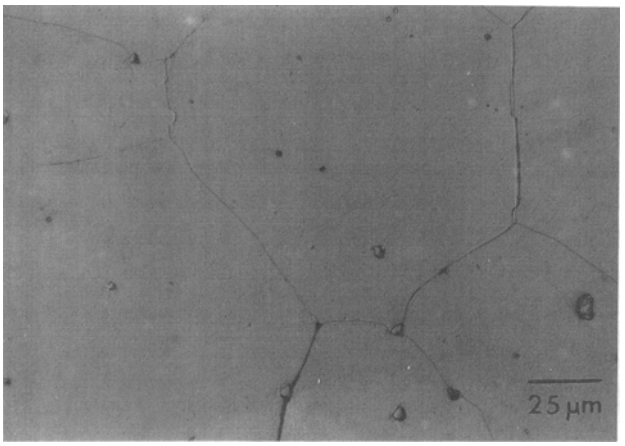

(*a*)

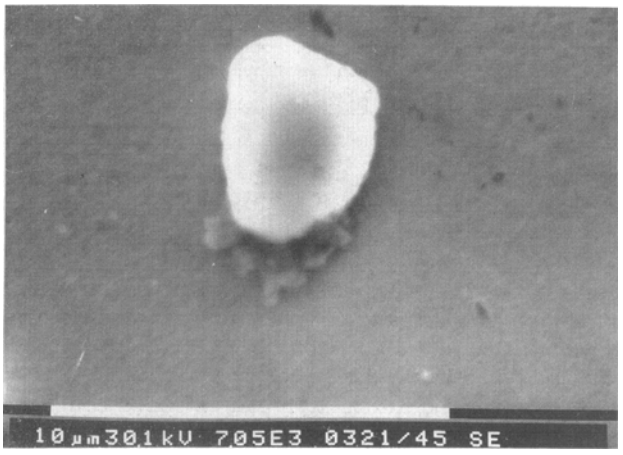

(*b*)

Fig. 11 — (*a*) Microstructure of alloy 1 homogenized for 15 min at 1093 °C, heated to a peak temperature of 1200 °C with thermocouple control, and quenched to room temperature. (*b*) Higher magnification microstructure of (a), showing the initiation of carbide liquation (L).

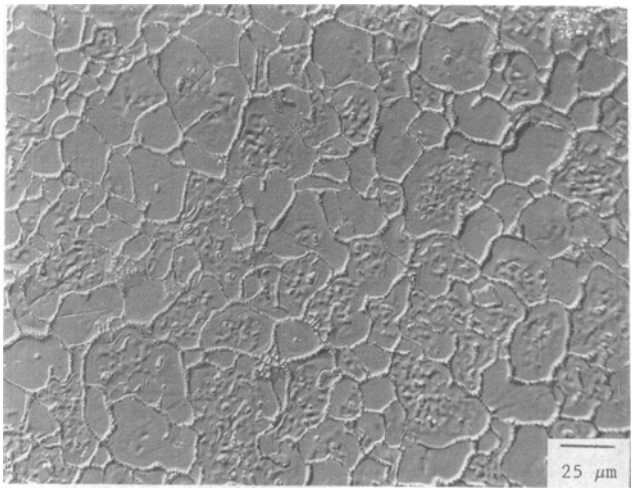

Fig. 12 — Alloy 1 in as-received condition heated to a peak temperature of 1227 °C using thermocouple control and quenched to room temperature. Notice the complete liquation of carbides, shown in Fig. 5(a).

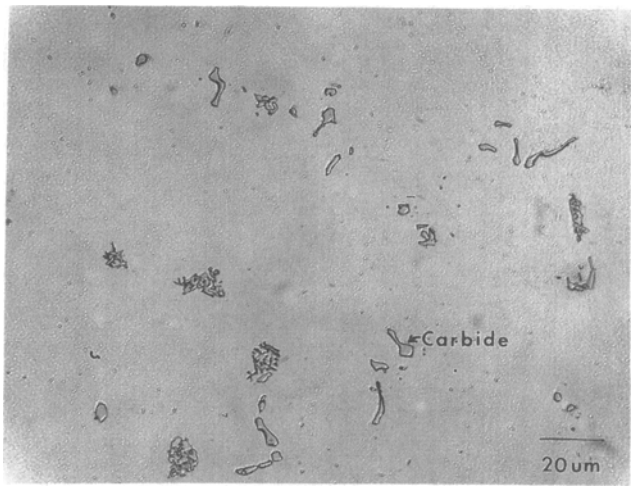

Fig. 13 — Microstructure of cast alloy 2 with a high C/Nb ratio prior to thermal cycling showing a high ratio of carbide/Laves phase.

could be obtained only by an isothermal hold at a peak temperature of 1235 °C. At a peak temperature of 1215 °C, the carbide appeared to be in equilibrium with a certain volume fraction of liquid and the matrix.

Second, the average concentration of the quenched-in liquid formed around the carbides in the wrought alloy (Figure 19 and Table IV) was approximately the same as that of the liquid giving rise to Laves phase in cast alloys.[13] This implies that the liquation of carbides in wrought alloys and Laves in cast alloys can be explained with the help of a common pseudo-ternary phase diagram (Figure 21).

A. *Microstructure-Phase Diagram Relationships*

The nominal composition of alloy 718 is such that a small quantity of carbide and Laves phase is stable at room temperature.[12] This requirement is satisfied by both alloys C_0 and C_1, shown in Figures 22 and 23, respectively. These are the vertical sections of the space diagram shown in Figure 21 through the planes 1-1 and 2-2,

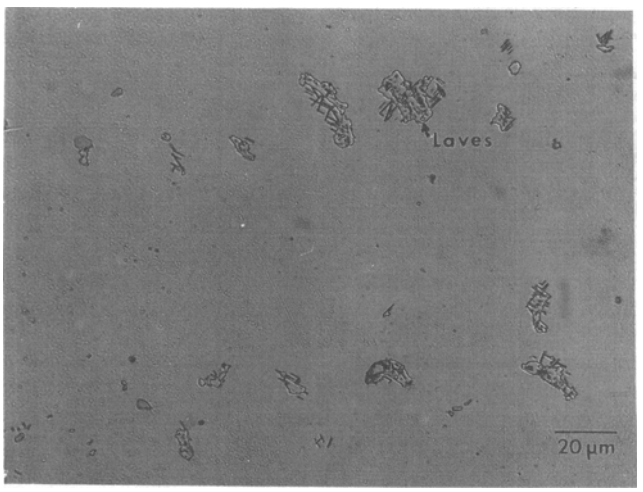

Fig. 14 — Microstructure of cast alloy 3 with a low C/Nb ratio prior to thermal cycling, showing a low ratio of carbide/Laves phase.

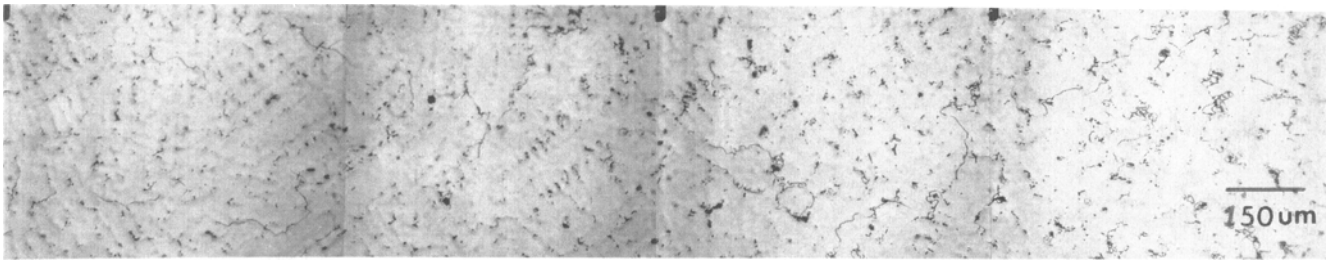

Fig. 15—Liquation in cast alloy 2 at various locations of the Gleeble sample quenched from 1235 °C. The extreme left corresponds to the beginning of liquation, and the extreme right corresponds to the liquation at 1235 °C.

respectively. When the alloys C_0 and C_1 are heated above the temperature T_{La}, shown in Figures 22 and 23, they enter the γ + NbC field. Hence, above this temperature, the Laves phase and a fraction of the carbides should dissolve. This is what happens during hot-working or heat-treating of alloy 718. On cooling from above T_{La}, reprecipitation of Laves phase and carbides generally does not occur because of their slow kinetics of formation. Hence, for both C_0 and C_1, the microstructure after thermal treating above T_{La} consists of NbC in a γ matrix.

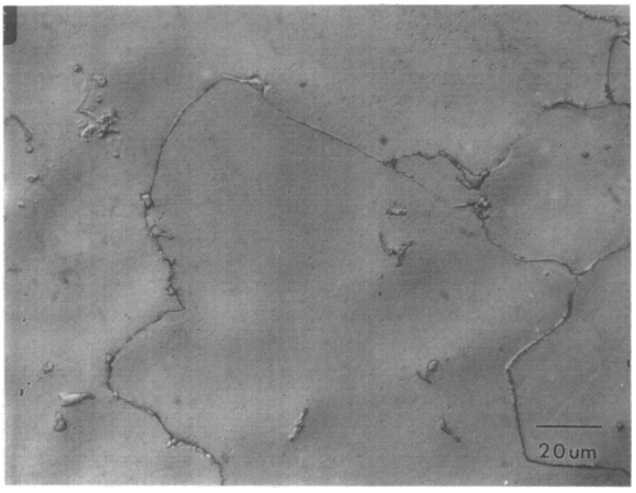

(*a*)

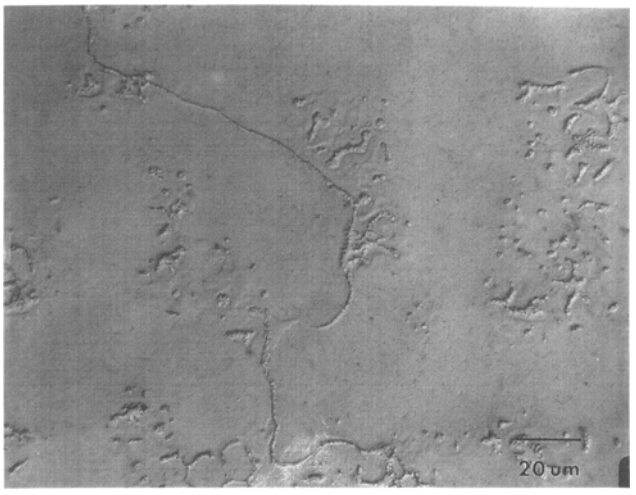

(*b*)

Fig. 16—(*a*) Liquation in cast alloy 2 quenched from a peak temperature of 1215 °C. (*b*) Liquation in cast alloy 3 when quenched from the same temperature. Alloy 3, with the larger prior volume fraction of Laves, shows the larger volume fraction of quenched-in liquid. Carbide liquation is insignificant at this temperature, as shown in (a) for alloy 2.

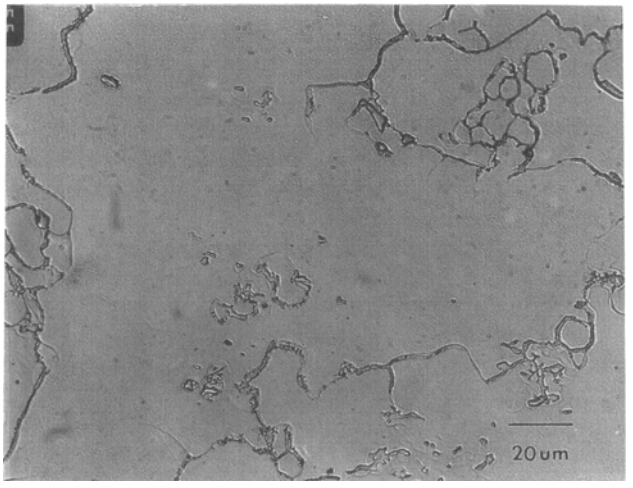

(*a*)

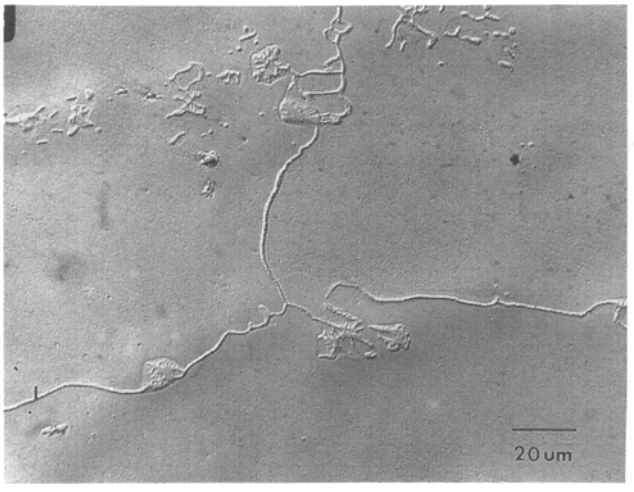

(*b*)

Fig. 17—Liquation of 1235 °C for (*a*) cast alloy 2 and (*b*) cast alloy 3. Notice the increase in the volume fraction of liquid for alloy 2 (compared to Fig. 16) due to the liquation of the carbides and no significant increase in the volume fraction of liquid in alloy 3 with low carbide content.

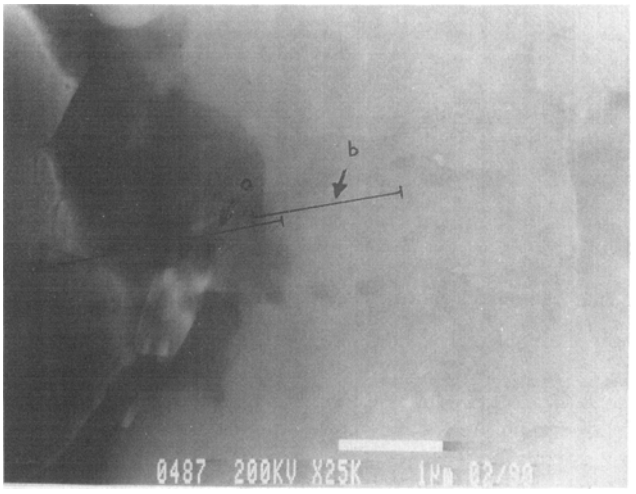

Fig. 18—Scanning transmission electron microscopy image of a liquating carbide in alloy 1, showing the liquation of carbide and the formation of liquid around the carbide. The straight lines marked "a" and "b" are the locations of the line scans shown in Figs. 19 and 20, respectively.

When the alloy C_0 is heated to the temperature T_C, the NbC particles should dissolve, since only γ is stable above this temperature. However, it is known in alloy 718 that NbC particles do not dissolve completely in the solid state. NbC particles were found to be stable up to 1205 °C on solution treating,[12,19] which is very close to the carbide liquation temperature shown in this study. Hence, the nominal composition of alloy 718 used in this study should correspond to compositions like C_1 shown in Figure 23, where the γ + NbC field is stable up to the temperature where the first incidence of liquation occurs on heating.

The alloy in the as-cast condition could contain a higher

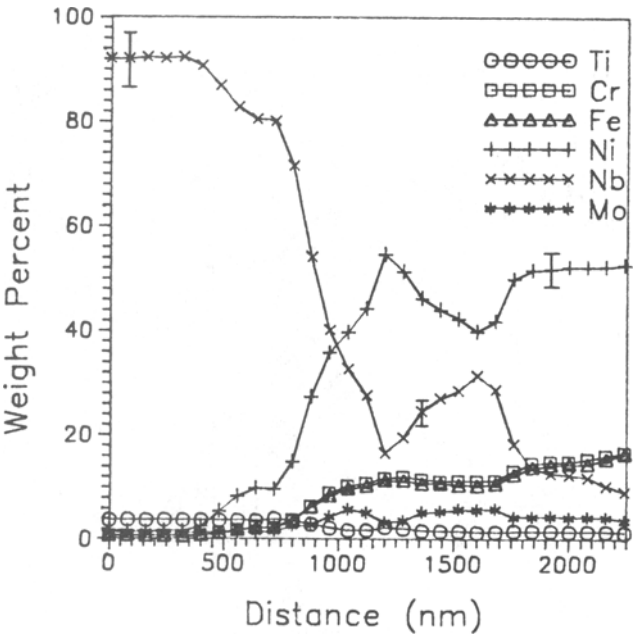

Fig. 19—Composition profile across the liquating carbide (line "a") shown in Fig. 18, covering the carbide, liquid, and matrix adjacent to the carbide. The errors bars represent the counting error only and do not include the error in the theoretical *k*-ratios.

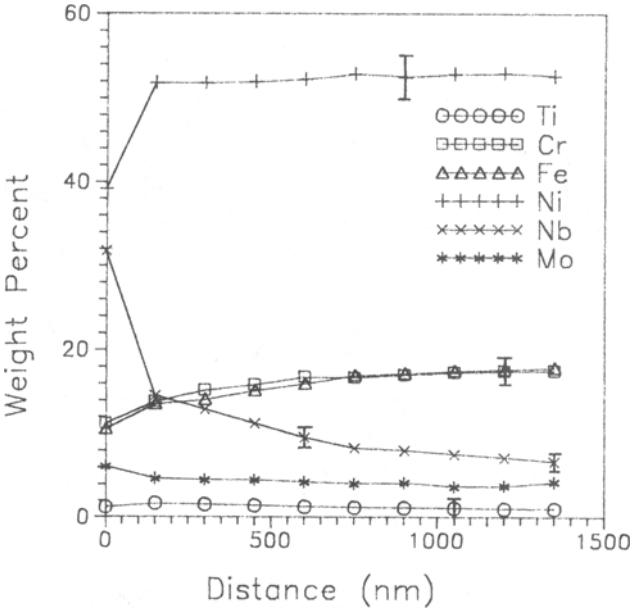

Fig. 20—Composition profile across the edge of the liquid and matrix adjacent to the liquid (line "b" in Fig. 18), showing the concentration gradient in the matrix adjacent to the liquid. The error bars represent the counting error only and do not include the error in the theoretical *k*-ratios.

volume fraction of carbide and Laves phase than what the phase diagram suggests because of coring during solidification. The relative volume fractions of NbC and Laves in the cast alloys of this study were seen to depend upon the C/Nb ratio. This can be explained with reference to the solidification paths for alloys 2 and 3 superimposed on the liquidus projection of the pseudo-ternary (Figure 24). Alloys with a high C/Nb ratio, such as alloy 2, will have a solidification path indicated by dotted line 2, whereas alloys with low C/Nb ratio, such as alloy 3, will have a solidification path shown by dotted line 3 in Figure 24. It is clear that the alloy with a solidification path given by dotted line 3 will have the lower volume fraction of carbide.

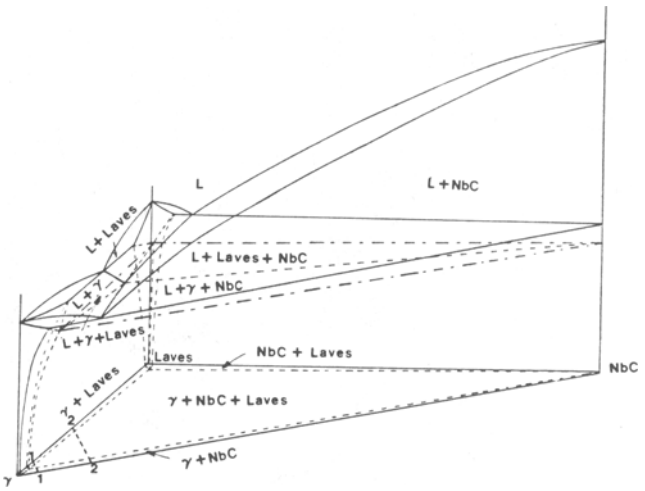

Fig. 21—Space diagram of the pseudo-ternary γ-NbC-Laves. The eutectic compositions and temperatures are represented schematically. 1-1 and 2-2 are traces of the vertical planes through the space diagram.

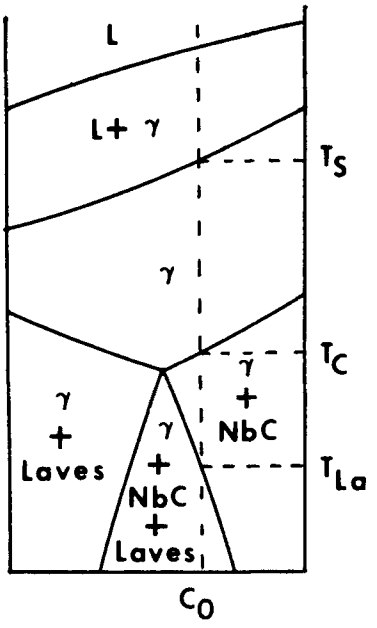

Fig. 22—Vertical section through the space diagram of Fig. 21 along 1-1. The term C_0 is the composition of an alloy which has a stable γ + NbC + Laves field at room temperature; T_{La} is the Laves dissolution temperature; T_C is the carbide dissolution temperature; and T_S is the γ solidus.

B. *Formation of NbC-γ Diffusion Couple in Wrought Alloy 718*

The wrought alloy (alloy 1) used in this study had an initial microstructure consisting of NbC and Ni_3Nb in a γ matrix. The precipitation of Ni_3Nb is obtained by heat-treating the homogenized alloy at a temperature of around 900 °C. If the solubility of NbC in the matrix at this

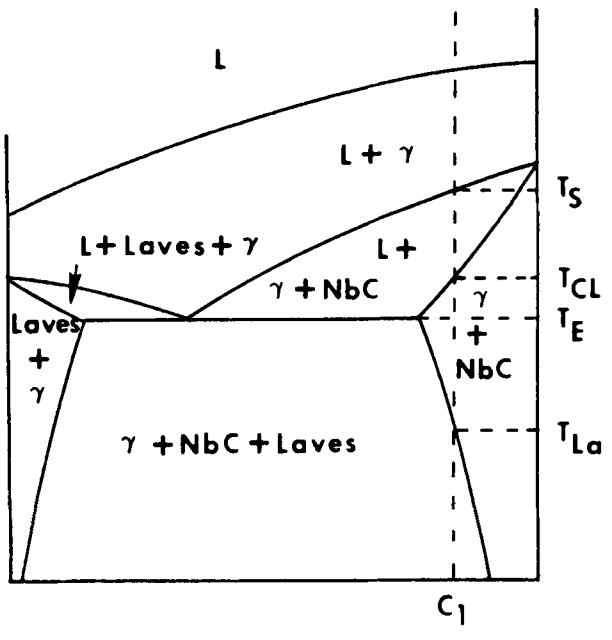

Fig. 23—Vertical section through the space diagram of Fig. 21 along 2-2. The term C_1 is the composition of an alloy having a stable γ + NbC + Laves field at room temperature; T_{La} is the Laves dissolution temperature; T_{CL} is the carbide liquation temperature; and T_S is the solidus temperature of the γ matrix.

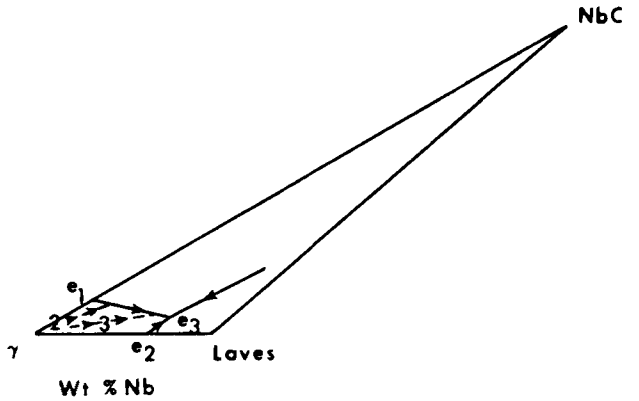

Fig. 24—Schematic of solidification paths for cast alloys 2 and 3. Alloy 2 with a high C-Nb ratio has a solidification path marked "2," which results in a high NbC/Laves ratio; alloy 3 with a lower C/Nb ratio has the solidification path marked "3," which results in a lower NbC/Laves ratio.

temperature can be neglected, then the initial matrix composition of alloy 1 in the as-received condition can be represented by C''_m, shown in Figure 25, which is an isothermal section through the pseudo-ternary space diagram at a temperature above T_E, the pseudo-ternary eutectic. This composition is raised to the point C'_m after the dissolution of the δ phase present in the as-received microstructure. It is known that the δ phase dissolves completely around 1010 °C. In the present study, the δ phase could be completely dissolved by a 100-second anneal at 1093 °C. Theoretically, there will also be a partial dissolution of the carbides during the homogenization heat treatment.[20,21] However, because of the short homogenization time used in this study (100 seconds), it is assumed that the matrix is not homogenized to a composition such as C_m. However, the following analysis will hold even if it is assumed that the matrix composition is homogenized to C_m as a result of the homogenization anneal. It is assumed, as mentioned earlier, that the composition of γ does not change during cooling from the homogenization temperature and that Laves phase and carbides do not precipitate on cooling from the homogenization temperature. Hence, at room

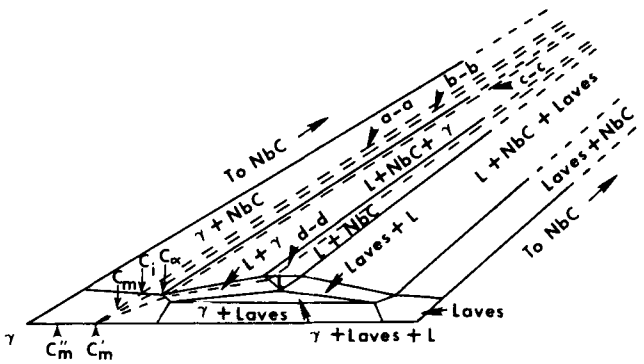

Fig. 25—Isothermal section through the space diagram of Fig. 21, just above the ternary eutectic. (*a*) The diffusion couple between NbC and the γ matrix of composition C_m is shown by the dotted line "a-a." The term C_i is the equilibrium matrix concentration at the NbC-matrix interface at this temperature; "b-b," "c-c," and "d-d" are possible diffusion paths between NbC and the matrix. C_α has the highest matrix Nb concentration that can exist at the NbC-matrix interface at the temperature of the isotherm.

temperature, the microstructure consists of a matrix of γ supersaturated with Nb, in equilibrium with NbC. When the alloy is rapidly heated to a temperature just above the pseudo-ternary eutectic, there will be a diffusion couple between NbC and the matrix. The formation of the diffusion couple is illustrated in Figure 25 by the dotted line "a-a." The diffusion couple must occur, since the matrix composition in equilibrium with NbC at the temperature of the isotherm, marked as C_i in Figure 25, has a higher Nb concentration than either C_m or C'_m due to the increased solubility of NbC in the matrix at the liquation temperature than the homogenization temperature. The evolution of the diffusion couple between NbC and the γ matrix of composition C'_m will be considered in the following section.

C. *Evolution of NbC-γ Diffusion Couple*

In order to understand the evolution of this diffusion couple, it is first necessary to look at the diffusion path in a binary diffusion couple. In a binary diffusion couple, the dissolution of a binary precipitate involves the transport of a single solute across the precipitate-matrix interface. The interface velocity in a binary diffusion couple is related to the solute flux across the moving interface as

$$R(C_{AB} - C'_B) = J_B \qquad [1]$$

where R is the interface velocity, C_{AB} is the solute concentration of the precipitate AB, C'_B is the solute concentration at the precipitate-matrix interface, and J_B is the solute flux across the interface. However, the dissolution of NbC in the γ matrix involves the simultaneous transport of Nb and C atoms across the NbC-γ interface. Hence, the flux equations for Nb and C should involve a common velocity term for the NbC-γ interface.[22] Hence,

$$R(C_{Nb} - C'_{Nb}) = J_{Nb} \qquad [2]$$

and

$$R(C_C - C'_C) = J_C \qquad [3]$$

where R is the interface velocity, C_{Nb} is the Nb concentration of the carbide, C_C is the carbon concentration of the carbide, C'_{Nb} is the Nb concentration of the matrix at the interface, and C'_C is the carbon concentration of the matrix at the interface. In Eqs. [2] and [3], it is assumed that the atomic volumes of Nb and C are constant in the carbide and the matrix, respectively. The flux of a component is related to its diffusivity through Fick's law. Hence,

$$J_{Nb} = -D_{Nb}dC_{Nb}/dx \qquad [4]$$

and

$$J_C = -D_C dC_C/dx \qquad [5]$$

Combining Eqs. [2] through [5],

$$(D_{Nb}dC_{Nb}/dx)/(C_{Nb} - C'_{Nb}) = (D_C dC_C/dx)/(C_C - C'_C) \qquad [6]$$

Hence, the diffusion path should be such that the interfacial Nb and C concentrations, C'_{Nb} and C'_C, satisfy Eq. [6].

The following three cases can be considered for the diffusion path between NbC and γ.

1. *Case 1: straight line path connecting NbC and C'_m*

In this case, carbide liquation will not occur at the temperature of the isotherm shown in Figure 25. The diffusion couple can operate entirely through solid state. The maximum interfacial Nb concentration would be given by the composition C_i shown in Figure 25. An approximate value for the interface composition C_i can be obtained as follows. The volume fraction of NbC in alloy 718 is typically about 1 wt pct. The Nb concentration in carbides is typically about 85 to 90 wt pct Nb. Assuming a typical matrix composition of about 5 wt pct Nb, even a complete dissolution of NbC in the solid state can raise the matrix Nb concentration to only about 5.5 to 6.0 wt pct Nb. Since complete dissolution of NbC does not occur in the solid state, the maximum Nb concentration in the matrix in equilibrium with NbC at the γ-NbC interface can only be marginally higher than 5.0 wt pct Nb. Carbide liquation can occur only at higher temperatures where the straight line diffusion path intercepts the γ-NbC-Laves triangle. From Figure 26, it is seen that the Nb concentration of the matrix in equilibrium with liquid cannot be much different from the Nb concentration at the matrix-NbC interface obtained at the lower temperature, since the L + NbC + γ triangle has to sweep to the left at higher temperatures in order to intercept the straight line diffusion path from NbC to γ.

2. *Case 2: deviation from straight line diffusion path within NbC + γ field*

In this case, the diffusion path is of the type "b-b" shown in Figure 25. The reason for the deviation from the straight line path "a-a" could be that the concentrations C'_{Nb} and C'_C represented by C_i do not satisfy Eq. [6]. Since the $D_{Nb} \ll D_C$, Eq. [6] could probably be satisfied by having an interface Nb concentration which is as close to C_{Nb} as possible. Interface Nb concentrations greater than C_i can be achieved if the diffusion path deviates

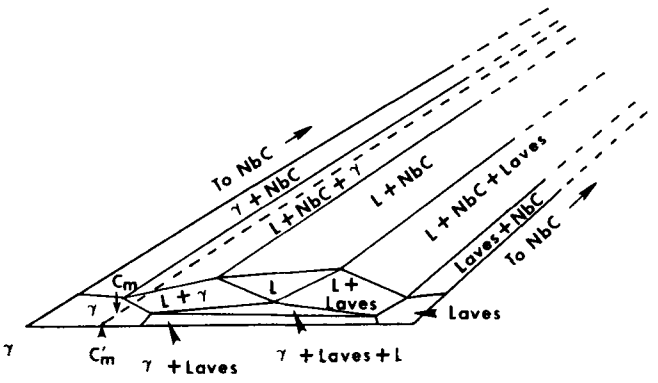

Fig. 26—Schematic of the isothermal section taken at a peak temperature higher than in Fig. 25. Notice that the temperature is such that the straight line connecting NbC and C'_m intersects the L + NbC + γ field. If a straight line diffusion path is assumed, then the interface composition between liquid and γ cannot be greater than the γ-NbC interface composition C_i shown in Fig. 25. This is because the L + NbC + γ triangle should sweep to the left in order to intersect the straight line joining NbC and γ.

from this straight line path and takes up paths of the type "b-b" in Figure 25, for which the interface compositions are situated to the right of C_i and, hence, represent greater Nb concentrations. Since the interface composition required to satisfy Eq. [6] is less than the composition $C\alpha$ shown in Figure 25, the diffusion couple can again operate in the solid state and there will be no carbide liquation at the temperature of the isotherm. However, liquation will occur at a higher temperature, since the concentration $C\alpha$ sweeps to the left at higher temperatures and it may not be high enough to satisfy Eq. [6]. However, the temperature at which liquation initiates will be lower than for case 1 above, where liquation initiates only at a temperature where the sweeping of the L + NbC + γ triangle to the left is high enough to intercept the straight line joining NbC and C'_m. The diffusion path at a temperature where carbide liquation initiates can be of the type marked "c-c" or "d-d" in Figure 25.

3. *Case 3: liquation diffusion path at any temperature above T_E*

If the composition $C\alpha$ is not high enough to satisfy Eq. [6] at any temperature above T_E, then the diffusion path for any temperature above T_E will be of the type "c-c" or "d-d" shown in Figure 25, and hence, carbide liquation occurs at a temperature as low as T_E. It must be mentioned here that the continued validity of Eqs. [4] and [5] for this case has the added assumption that Nb and C do not interact with the other components in the liquid.

D. *Constitutional Nature of Carbide Liquation*

In both cases 2 and 3 described above, the interface between liquid and matrix should support a higher Nb concentration than in case 1. In the present study, the matrix in contact with liquid has been found to be enriched in Nb to about 9 to 11 wt pct Nb. Since the interface composition for a straight line diffusion path, C_i, can be only marginally higher than 5.0 wt pct Nb, a Nb concentration of 9 to 11 wt pct is possible only if the evolution of the γ-NbC diffusion couple occurs through a diffusion path involving tie lines which do not pass through the average composition C_0, according to cases 2 and 3 above. These tie lines, however, represent local equilibria at the carbide-liquid and liquid-matrix interfaces.

In cases 2 and 3 above, liquation of carbides due to the diffusion path represented by either "c-c" or "d-d" should be constitutional in nature, since at equilibrium, the alloy composition C_0 lies in the γ + NbC field. Continued holding at the peak temperature would therefore result in the complete disappearance of the liquid. Isothermal liquation studies[18] do indicate a reduction in the volume fraction of liquid as a function of isothermal hold time, at temperatures where the liquation of the carbides just initiate. At a peak temperature of 1200 °C, where carbide liquation initiated, it appeared that the initial liquid was completely removed by an isothermal hold. At a peak temperature of 1215 °C, NbC, γ, and a small volume fraction of liquid appeared to coexist after an isothermal hold. Hence, this temperature would probably correspond to the temperature T_{CL} marked in Figure 23. At a peak temperature of 1190 °C, no liquid was detected. Hence, the ternary eutectic temperature is probably between 1190 °C and 1200 °C. These temperatures are marked in Figure 23.

In order to determine whether the diffusion path "c-c" or "d-d" is operative, the morphology of carbide liquation should be examined. Figure 27 shows the expected liquation morphologies for the two diffusion paths.[23] Our experience with the liquation microstructures suggests that the diffusion path "d-d" could be operative. For the diffusion path "d-d," the movement of the interface between NbC and liquid will be governed by the diffusivities of Nb and C in liquid, which, unlike in the solid state, are not very much different (assuming no interaction between components). Hence, it may be possible for the system to choose a tie line in the NbC + L region which will satisfy Eq. [6].

Hence, the existence of a complex diffusion path explains constitutional liquation of NbC above the terminal ternary eutectic. The resulting liquid resolidifies according to the phase diagram requirements and forms essentially Laves phase and a small fraction of eutectic carbide.

E. *Effect of Peak Temperature on the Extent of Constitutional Liquation*

For both cases 2 and 3 described above, it can be seen that the initial tie line that the system chooses during dissolution of NbC does not pass through the average

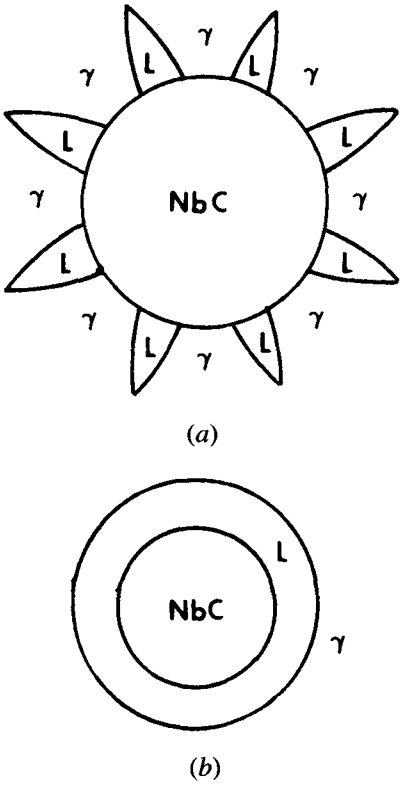

Fig. 27—Expected morphology of carbide liquation for the diffusion paths given by (*a*) c-c and (*b*) d-d. Notice that the diffusion path c-c involves three-phase equilibrium, and the volume fractions of liquid and γ decrease as a function of distance from the edge of the carbide. Hence, the star-shaped morphology should be obtained. However, the diffusion path d-d does not involve three-phase equilibrium, and hence, a planar interface is possible between NbC and liquid. Also, the liquid can completely surround the carbide.

composition C_0. However, if the peak temperature (above T_E) is such that the average composition C_0 lies in the NbC + γ region, then the volume fraction of NbC in equilibrium with γ at that peak temperature will be given by the tie line in the NbC + γ field passing through C_0. In this case, all of the initial liquid produced by constitutional liquation would be metastable and would disappear upon continued isothermal hold at the peak temperature. At a higher peak temperature where C_0 lies in the L + NbC + Laves field, the final volume fraction of NbC, liquid, and Laves phase in equilibrium would be given by the appropriate tie triangle. Here, part of the initial liquid would be metastable, because nonequilibrium concentration gradients in the liquid and solid would cause an excess in the quantity of the initial liquid. Since the composition C_0 is such that complete dissolution of NbC would not occur in the solid state, the equilibrium path of C_0 goes through γ + NbC, L + NbC + γ, and L + γ as the temperature is increased. However, the initial formation of metastable liquid above the terminal eutectic temperature, according to either case 2 or 3 above, is due to the kinetic factors related to the diffusion fluxes of Nb and C described earlier.

F. *Comparison of Pseudo-Binary (c-Laves) and Pseudo-Ternary (c-NbC-Laves) Approaches to Alloy 718*

The terminal eutectic of γ + NbC + Laves in the present analysis actually corresponds to the γ + Laves pseudo-binary terminal eutectic reported by several authors.[12,13,14] The true binary γ-Laves eutectic (which is represented as one of the binaries of the pseudo-ternary model) is not known. The pseudo-binary eutectic reported in the literature for alloy 718 shows up as a terminal reaction peak during thermal analysis. It is known that the products of terminal solidification actually contain several minority phases such as carbides, borides, carbosulfides, *etc.*,[16] in addition to γ and Laves, although the volume fractions of these minority phases are quite insignificant. In the present analysis, the terminal solidification is simplified as a γ, Laves, NbC eutectic, since this is one of the thermodynamically permissible ways to end the monovariant reaction, L → NbC + γ,[15] which is known to occur in this alloy.[13]

The lowest temperature at which a stable liquid can form from carbide liquation in alloy 718 corresponds to T_{CL}, which was 1215 °C in the alloy under study (Figure 23). This should correspond to the true solidus of the alloy in a pseudo-ternary representation. Pseudo-binary representations of alloy 718 require that the solidus temperature correspond to entering the L + γ field and thus require complete carbide liquation. This occurred at a peak temperature of 1227 °C to 1235 °C in the present study. Isothermal liquation studies[18] showed that a certain fraction of the initial liquid produced at this temperature was stable. This then would correspond to the solidus temperature in the pseudo-binary representation. This is in close agreement with the temperature of 1227 °C reported by Eiselstein[12] for the solidus temperature and is marked as T_S in Figure 23. Knorovsky *et al.*[13] reported a temperature of 1250 °C for the beginning of carbide formation during cooling. In the pseudo-ternary representation, 1250 °C corresponds to the beginning of the monovariant L → γ + NbC reaction, which also corresponds to the temperature marked T_S in Figure 23. It is interesting to note that this temperature, T_S, ranges from 1232 °C to 1260 °C for the four different heats used by Knorovsky *et al.*[13] This would be expected for a monovariant reaction, as represented in Figure 23.

G. *Liquation by Solute Enrichment*

The wrought alloy used in this study was in the form of hot-rolled rods approximately 5 mm in diameter. Because of a large reduction during the hot-working process, some of the solidification carbides can fracture. This results in a large size distribution of the carbides in wrought products. The volume fraction of NbC in the wrought alloy prior to the weld thermal cycle is determined by the tie line relationships that exist in the γ + NbC field during the homogenization heat treatment in the Gleeble. It is possible that some of the fine carbides situated along grain boundaries completely dissolve during the homogenization treatment. It is known that the dissolution of these grain-boundary precipitates can result in a local enrichment of the grain boundaries.[24,25] Upon subsequent heating to higher temperatures in the Gleeble, further dissolution of some of the bigger carbides might take place in the temperature range of T_H to T_E, where T_H is the homogenization temperature and T_E is the ternary eutectic temperature, because of the greater solubility of the carbides at T_E compared to T_H. The extent of solute enrichment occurring on the grain boundaries depends on the diffusion path in the γ + NbC field, as explained earlier. On heating further to a temperature above T_E, the composition of γ at these prior NbC locations may temporarily fall in the L + γ field and produce constitutional liquation. Hence, at temperatures where the NbC is constitutionally liquating because of the action of the diffusion couple (Figure 25), the solute-rich regions resulting from dissolution of fine carbides at lower temperatures may also constitutionally liquate independent of the carbides. This is one explanation for liquation in regions remote from carbides (Figures 7 through 9). This phenomenon is generally observed along grain boundaries where enhanced diffusion allows for rapid dissolution of smaller carbides. Part of this liquation could also be due to the solute enrichment that could arise due to incomplete homogenization following dissolution of Ni_3Nb present in the as-received alloy. However, isothermal liquation studies[18] indicated that these regions homogenized without liquation at temperatures where carbide liquation just initiated (1200 °C to 1215 °C). At higher temperatures (1227 °C), these regions appeared to liquate prior to homogenization. In the present study, it is possible that such a liquation occurred at the center of the Gleeble sample (Figure 9), where the peak temperature was 1227 °C to 1235 °C.

The presence of an etching relief adjacent to the liquating grain-boundary carbides and also around the liquating interior carbides (Figure 7) is due to a Nb diffusion gradient in the alloy matrix. This gradient arises because of a diffusion couple between NbC and the γ matrix at a temperature where the dissolution of the carbide occurs

through the liquid. The concentration of γ in equilibrium with liquid is given by $C\alpha$ (Figure 25). In the present study, the Gleeble samples were quenched to room temperature in order to retain the high-temperature microstructure resulting from the evolution of the NbC-γ matrix diffusion couple. However, the liquid undergoes a transformation during quenching and results in the formation of a divorced eutectic of NbC, Laves, and γ. The Nb concentration of γ formed as a divorced eutectic has been shown to be about 9.3 pct Nb.[13] In the present study, the maximum Nb concentration of the matrix in contact with the Laves phase is about 11 to 12 wt pct Nb. The Nb concentration of the Laves phase is about 30 wt pct Nb compared to a value of about 23 wt pct Nb reported by Knorovsky *et al.*[13] It is significant to note that there is a concentration gradient in the matrix ranging from about 11 wt pct Nb close to the Laves phase to about 6.5 wt pct Nb at a distance of about 1 μm from the Laves phase. This concentration gradient indicates the operation of the diffusion couple described earlier.

The Nb concentrations of NbC, Laves, and γ obtained in the present study by EDS on TEM foil are consistently greater than the values reported by Knorovsky *et al.*[13] As mentioned earlier, it should be noted that the absolute concentration values reported in the present study are not accurate because of the errors in quantification as a result of using theoretically calculated *k*-ratios and insufficient counting, especially for matrix Nb content away from the carbide-matrix interface. However, the absolute values of the concentrations are not important here. What is important is the fact that there is a relative Nb concentration gradient in the matrix justifying the presence of a diffusion couple between NbC and the matrix. Also, the magnitude of the matrix Nb concentration gradient justifies the assumption of a complex diffusion path between NbC and the matrix.

H. *Liquation in Cast Alloys*

It can be readily seen from the pseudo-ternary diagram that liquation of the Laves phase initiates at the pseudo-ternary eutectic temperature. However, since the position of the pseudo-ternary eutectic is such that very little eutectic carbide forms, the contribution of the carbides to the formation of liquid at temperatures just above the pseudo-ternary eutectic would be very small. It can be seen from Figure 16 that at a peak temperature of 1215 °C, liquation is quite insignificant in alloy 2, in which the carbide/Laves ratio in the as-cast microstructure was high. However, liquation is quite extensive for alloy 3 at the same peak temperature, since the carbide/Laves ratio was higher than in alloy 2. Figure 17 shows that the quantity of liquid increases considerably in alloy 2 at a peak temperature of 1235 °C due to the contribution from carbides. However, in alloy 3, the volume fraction of liquid does not increase appreciably because of the smaller volume fraction of carbides in the initial microstructure.

V. CONCLUSIONS

1. Both the constitutional liquation of carbides in wrought alloys and the eutectic melting of the Laves phase in the cast alloys can be explained with the help of the γ-NbC-Laves pseudo-ternary representation of alloy 718.
2. Constitutional liquation of NbC occurs in wrought alloy 718 at temperatures above the pseudo-ternary eutectic temperature but below the equilibrium γ + NbC $\rightarrow$ L + γ + NbC transition temperature for the nominal composition of alloy 718. This is due to the evolution of a diffusion couple between NbC and the γ matrix through a diffusion path which deviates from the straight line path connecting the terminal compositions.
3. Part or all of the initial liquid produced during rapid heating is metastable depending upon the peak temperature of the thermal cycle.
4. Constitutional liquation in wrought alloy 718 may also occur by the dissolution of fine carbides during rapid heating up to the pseudo-ternary eutectic temperature and subsequent liquation of the solute-enriched regions at higher temperatures.
5. In cast alloy 718, liquation initiates at the pseudo-ternary eutectic.
6. At temperatures just above the pseudo-ternary eutectic temperature, the volume fraction of liquid is determined by the volume fraction of Laves phase in the initial microstructure since the position of ternary eutectic is such that there is very little eutectic carbide.
7. At higher peak temperatures, carbides liquate readily and contribute to the liquid.

ACKNOWLEDGMENTS

The authors wish to acknowledge the useful discussions with Dr. J.B. Andrews of the University of Alabama at Birmingham and Dr. C.L. White of Michigan Technological University, Houghton, MI, on diffusion couples in ternary systems. They also acknowledge the support given to this research by the National Science Foundation under Grant No. DMR-8807915.

REFERENCES

1. D.S. Duvall and W.A. Owczarski: *Weld. J.*, Sept. 1967, vol. 46 (9), pp. 423s-432s.
2. B. Weiss, G.E. Grotke, and R. Stickler: *Weld. J.*, Oct. 1970, vol. 49 (10), pp. 471s-487s.
3. J.J. Pepe and W.F. Savage: *Weld. J.*, Dec. 1970, vol. 49 (12), pp. 545s-553s.
4. J.A. Brooks: *Weld. J.*, Nov. 1974, vol. 53 (11), pp. 517s-523s.
5. W.A. Baeslack III, S.J. Savage, and F.H. Froes: *J. Mater. Sci. Lett.*, 1986, pp. 935-39.
6. J.J. Pepe and W.F. Savage: *Weld. J.*, Sept. 1967, vol. 46 (9), pp. 411s-422s.
7. R.G. Thompson and S. Genculu: *Weld. J.*, Dec. 1983, vol. 62 (12), pp. 337s-345s.
8. W.A. Baeslack III and D.E. Nelson: *Metallography*, 1986, vol. 19, pp. 371-79.
9. P.J. Valdez and J.B. Steinman: *Effect of Minor Elements on the Weldability of High-Nickel Alloys*, Welding Research Council, New York, NY, 1969, pp. 93-120.
10. E.G. Thompson: *Weld. J.*, Feb. 1969, vol. 48 (2), pp. 70s-79s.
11. T.J. Kelly: *Trends in Welding Research*, ASM, Metals Park, OH, 1986.
12. H.L. Eiselstein: *Advances in the Technology of Stainless Steels*

and Related Alloys, ASTM STP 369, ASTM, Philadelphia, PA, 1965, pp. 62-79.
13. G.A. Knorovsky, M.J. Cieslak, T.J. Headley, A.D. Romig, and W.F. Hammetter: *Metall. Trans. A*, 1989, vol. 20A, pp. 2147-56.
14. G.K. Bouse: *Superalloy 718 Metallurgy and Applications*, TMS, Warrendale, PA, 1989, pp. 69-77.
15. B. Radhakrishnan and R.G. Thompson: *Metall. Trans. A*, Dec. 1989, vol. 20A, pp. 2866-68.
16. R. Vincent: *Acta Metall.*, July 1985, vol. 33 (7), pp. 1205-16.
17. D.B. Williams: *NORELCO Reporter*, 1982, vol. 29 (3), pp. 6-41.
18. B. Radhakrishnan and R.G. Thompson: *Recent Trends in Welding Science and Technology, TNR '89*, ASM INTERNATIONAL, Metals Park, OH, 1990, pp. 637-48.
19. J.M. Poole, K.R. Stultz, and J.M. Manning: *Proc. Int. Symp. on the Metallurgy and Applications of Superalloy 718*, Pittsburgh, PA, June 12–14, 1989, TMS, Warrendale, PA, 1989, pp. 219-28.
20. B. Radhakrishnan and R.G. Thompson: *Metallography*, 1988, vol. 21, pp. 453-71.
21. D. Mayo: Masters Thesis, University of Alabama at Birmingham, Birmingham, AL, 1987.
22. J.S. Kirkaldy and D.J. Young: *Diffusion in the Condensed State*, The Institute of Metals, London, 1987, p. 366.
23. J.B. Clark: *Trans. TMS-AIME*, 1963, vol. 227, pp. 1250-51.
24. A. Pasparakis, D.E. Coates, and L.C. Brown: *Acta Metall.*, 1973, vol. 21, pp. 991-1001.
25. A.D. Romig, Jr., J.C. Lippold, and M.J. Cieslak: *Metall. Trans. A*, 1988, vol. 19A, pp. 35-50.